Density Functional Theory Calculations on EOS and Phase Stability of Beryllium

Sven P. Rudin

Sven P. Rudin(1), M. D. Jones(2), and J. D. Johnson(1),*

(1)Theoretical Division, Los Alamos National Laboratory, Los Alamos, NM 87544, USA

(2)Center for Computational Research, University at Buffalo, The State University of New York, Buffalo, NY 14260, USA

**corresponding author: srudin@lanl.gov*

Abstract

Our current equation of state (EOS) for Beryllium is based on experimental data and empirical models. This construction does not fully constrain the resulting EOS, and recently uncovered experimental results in the literature show slight disagreement with the established EOS of Be. To address this disagreement we have calculated the cold curve and the phonons for Be in the hexagonal close-packed (hcp) structure using density functional theory. From these we extract the thermal expansion and the Grüneisen parameter; the former agrees well with experiment, the latter leads to a slight adjustment of the EOS. The same calculations for Be in the body-centered cubic (bcc) structure leads to a predicted structural phase transition from hcp to bcc at a pressure of 415 GPa (at 0 K) that decreases to 360 GPa (near the melting temperature T_m=1560 K).

Introduction

Beryllium has a simple atomic configuration with four *s* electrons. The energy of the 2*p* states lies in close proximity to that of the 2*s* states, which results in several anomalies in the solid state, such as a Poisson ratio of only 0.05 and an unusually high Debye temperature of 1440 K. At ambient pressure Be remains in the hexagonal close packed (hcp) crystal structure up to temperatures close to melting at 1560 K, transforming into the body-centered cubic (bcc) structure at 1530 K. The hcp crystal is far from ideal with a *c/a* ratio of 1.568 at ambient conditions.

The zero temperature isotherms (Lyon *et al.*, 1998) that were originally derived from the experimental shock Hugoniot (Marsh, 1980) are calculated from the Mie-Grüneisen reduction of the Hugoniot data (McQueen *et al.*, 1970). For zero to room temperature corrections the thermal equation of state was from the Debye phonon model with a minor contribution from the electronic specific heat. For this analysis the Grüneisen parameter □ as a function of density □ is required. The initial modelling used a form for □ that is quadratic in the inverse density □ with the values □=1.7 and *d*□/*d*(ln □)=-1 at ambient pressure and temperature as well as the limiting value of □=2/3 for □□ . This is reasonable and standard modelling but it does not match more recent diamond anvil data (Velisavljevic *et al.*, 2002). To obtain agreement with this data, it would be necessary to have a peak in □ (a value of 1.965 at □=2.96 g/cm^3).

Such a peak in the form of the Grüneisen parameter as a function of density is quite unlikely. This motivated the DFT study of beryllium presented here, which also aimed to address a second discrepency: Under compression beryllium is predicted theoretically to transform from the hcp to the bcc (and perhaps the fcc) crystal structure at a pressure between 100 GPa and 200 GPa (McMahan, 1982; Lam *et al.*, 1984). Experimentally this transition has not been observed up to a maximum (static) pressure of 171 GPa (Ming and Manghani, 1984; Olijnyk and Jephcoat, 2000; Nakano *et al.*, 2002, Velisavljevic *et al.*, 2002).

Methodology

Electronic structure calculations were performed with three different density functional theory (DFT) augmented wave methods. The methods have been extensively used as well as described in the literature (see references in the following three paragraphs); here we touch only on the main differences and common points. All methods partition real space into a spherical region around the atomic nucleus and an interstitial region but with differing representations of the electronic density. The reported calculations are scalar-relativistic, neglecting spin-orbit coupling for the valence electrons. The parameters controlling convergence were chosen to assure convergence.

(1) The self-consistent full potential linear muffin-tin orbital (FP-LMTO) method (Wills and Cooper, 1987; Wills *et al.*, 2000) uses radial basis functions inside the nucleus-centered, spherical region (muffin-tin spheres). These are linear combinations of radial wave functions and their energy derivatives; outside the muffin-tin spheres the basis functions are combinations of Neuman or Hankel functions. The sphere is scaled with volume so that it always has a ratio of 0.758. Both the 1*s* and 2*s* electrons were treated as valence electrons, and the electron exchange-correlation was treated in the generalized gradient approximation (GGA) known as PBE96 (Perdew *et al.*, 1996).

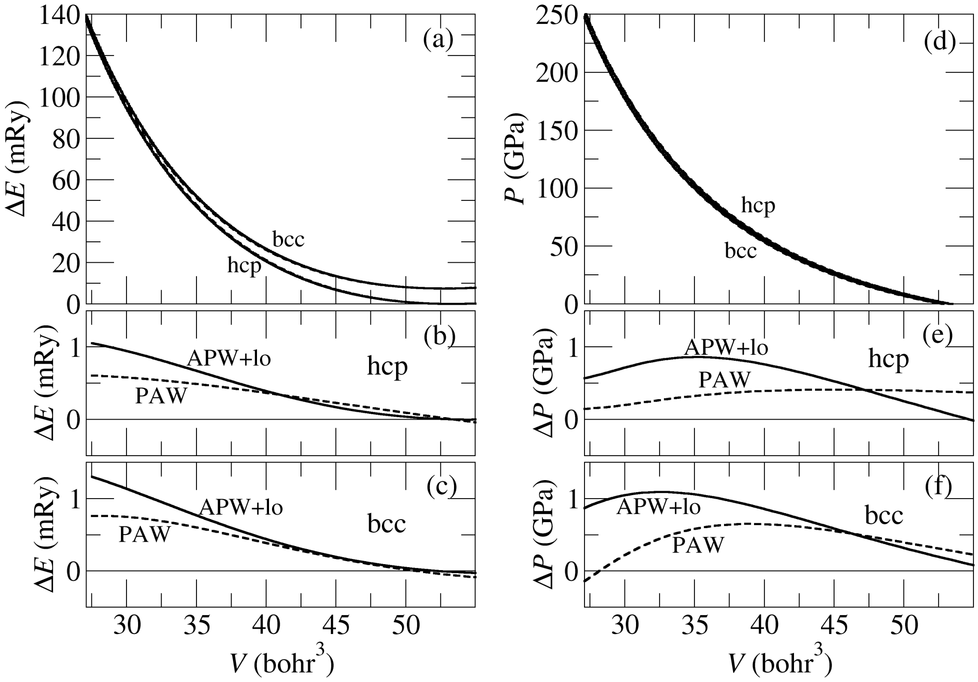

Figure 1. Cold curves for Be in the hcp and bcc structures using the three methods. (a) Energies for beryllium in the hcp and bcc structures plotted relative to the minimal energy of the hcp structure. (b) Differences in the total energies of the hcp structure relative to the results calculated with the FP-LMTO method. (c) Differences in the total energies of the bcc structure relative to the FP-LMTO results. (d) Calculated pressure for beryllium in the hcp and bcc structures. (e) Differences in the pressure of the hcp structure relative to the FP-LMTO results. (f) Differences in the pressure of the bcc structure relative to the FP-LMTO results.

(2) The projector-augmented wave (PAW) method (Blöchl, 1994) implemented in VASP (Kresse and Furthmüller, 1996; Kresse and Joubert, 1999) uses a superposition of a plane wave basis set in the interstitial region with atomic and pseudo atomic orbitals in the nucleus-centered region, which has a constant radius of 1.8 a_0. Brillouin zone integrations were done

with the improved tetrahedron method (Blöchl *et al.*, 1994). Both the 1s and 2*s* electrons were treated as valence electrons; the calculations use the generalized gradient approximation (GGA) known as PW91 (Perdew, 1991).

(3) The all-electron, full potential augmented plane wave plus local orbital (APW+lo) method as implemented in WIEN2k (Blaha *et al.*, 2001) uses linear combinations of radial functions multiplied by spherical harmonics inside the sphere (of constant radius 1.374 a_0; 1.7 a_0 for the phonon calculations) and plane waves in the interstitial region. Brillouin zone integrations were done using the improved tetrahedron method (Blöchl *et al.*, 1994). The calculations use the generalized gradient approximation (GGA) known as PBE96 (Perdew *et al.*, 1996). In contrast to the FP-LMTO and PAW calculations the APW+lo 1*s* electrons are treated as core states.

Figure 1 compares the cold curves of Be calculated with the three electronic structure methods. The differences for both hcp and bcc crystal structures are negligible near the experimental equilibrium volume and remain quite small under compression. The calculated hcp bulk modulus at equilibrium is consistent among the three methods ($B_{\text{FP-LMTO}}$=121 GPa, B_{PAW}=120 GPa, $B_{\text{APW+lo}}$=123 GPa) but somewhat smaller than the experimental value (B_{exp}=130 GPa); similar agreement is found for the hcp equilibrium volume ($V_{\text{FP-LMTO}}=53.3\ a_0^3$, $V_{\text{PAW}}=53.5\ a_0^3$, $V_{\text{APW+lo}}=53.3\ a_0^3$, $V_{\text{exp}}=54.7\ a_0^3$).

The phonons were calculated with the direct force method (Kunc and Martin, 1982; Wei and Chou, 1992; Frank *et al.*, 1995; Parlinski *et al.*, 1997). This method requires large simulation cells consisting of repeated unit cells. In these large simulation cells the force constants are evaluated from the forces on all atoms calculated in response to the displacement of a basis atom in one unit cell. The force constants are Fourier transformed with a given wave vector **q**, resulting in the **q**–dependent dynamical matrix, which upon diagonalization gives the corresponding phonon frequencies.

The evaluation of the force constants using small atomic displacements (i.e., remaining in the harmonic regime) for each crystal structure at a sequence of volumes leads to the resulting phonon frequencies being volume dependent (quasiharmonic approximation), which implicitly includes some anharmonic contributions. The calculations are therefore most accurate at low temperatures but less reliable at temperatures near melting because of missing high-temperature anharmonic contributions. Melting itself is nonexistent in the quasiharmonic approximation.

Extracting the Gibbs free energy from the calculations involves integrating over the phonon density of states (DOS) as well as the electronic DOS (Pathria, 1972). The latter, evaluated from the electronic DOS that each code generates, plays a negligible role. The phonon DOS is obtained by calculating the vibrational frequencies on a mesh in reciprocal space, with the mesh chosen to be fine enough to guarantee convergence.

Results

The calculation of the Grüneisen parameter $\square$ as a function of density $\square$ rests on evaluating the phonons and their logarithmic phonon moment $\square_0$ for a sequence of volumes. Within this procedure we make two comparisons with experimental data that are independent of the shock data: the phonon dispersion in the hcp structure at equilibrium and the thermal expansion. The comparisons (shown in Figs. 2 and 3) give some confidence that the DFT calculations, while not perfect, are accurate enough to investigate the presence or absence of an anomaly in the Grüneisen parameter.

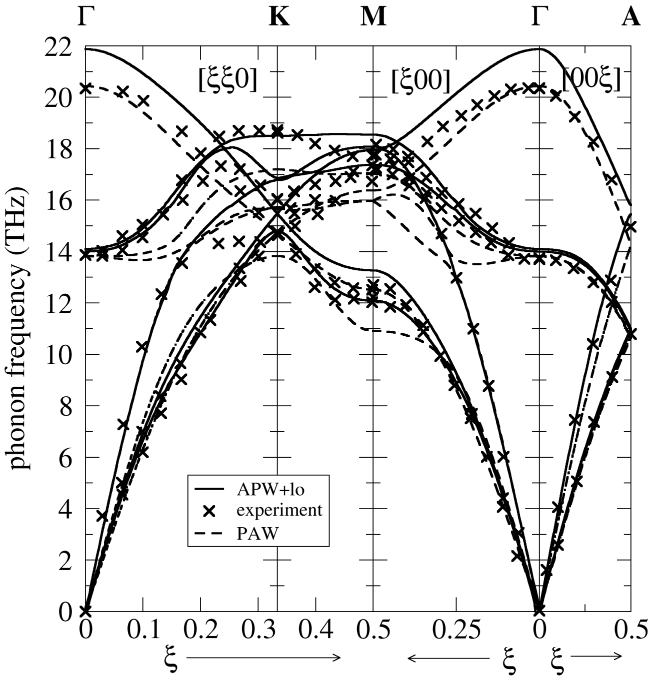

Figure 2. Calculated and experimental phonon dispersions at the experimental volume and c/a ratio. The acoustic branches show excellent agreement between experimental and calculated phonon frequencies. The differences in the optical branches between the two methods are of the same magnitude as the differences between either method and experiment.

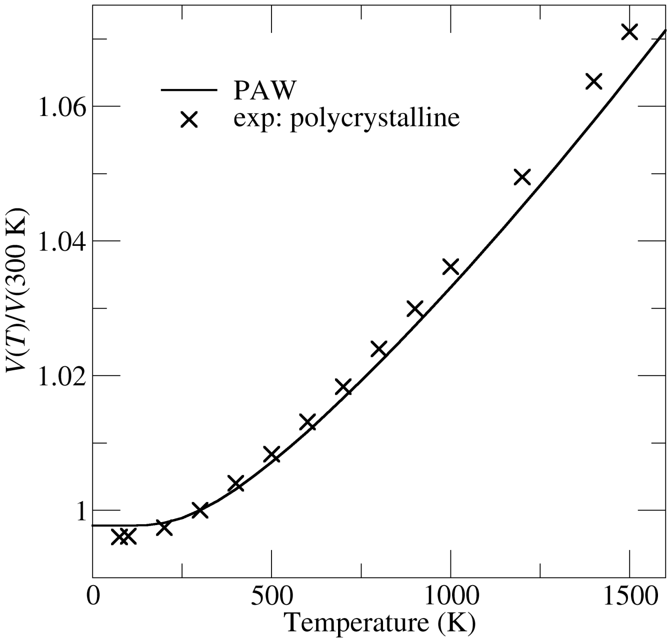

Figure 3. Thermal expansion of hcp Be. The ratio of theoretical to experimental equilibrium volume (at 300 K) is 0.977 for the cold curve and improves to 0.995 when the zero point energy of the calculated phonons is included.

Based on the phonon DOS we have evaluated the logarithmic phonon moment $\Box_0$ for both the hcp and bcc crystal structures (see Fig. 4a). At each volume the $\Box_0$ for the bcc structure lies lower than that for the hcp structure; similarly, plotting the moments as a function of pressure does not change this ordering. This suggests that an increase in temperature will lower the Gibbs free energy of the bcc structure more rapidly than that of the hcp structure.

The average phonon frequency provides a measure for how much thermal energy Be can absorb. How this measure changes with volume determines the thermal part of the EOS and is quantified in the Grüneisen parameter Γ. The Grüneisen parameter is given by the (logarithmic) derivative of θ_0 with respect to decreasing volume. The phonon moments are fit to a functional form chosen such that the Grüneisen parameter depends linearly on the volume and tends to 2/3 in the limit of infinite density.

Figure 4b shows the resulting Grüneisen parameter in comparison with the original EOS model as well as the experimental data point at equilibrium density. The differences are reasonably small, a slight change in the model (now termed `refit EOS model') improves the agreement with only negligible increases in the differences obtained for other variables such as the cold curves. The DFT results show no evidence of any anomalous behavior of the Grüneisen parameter.

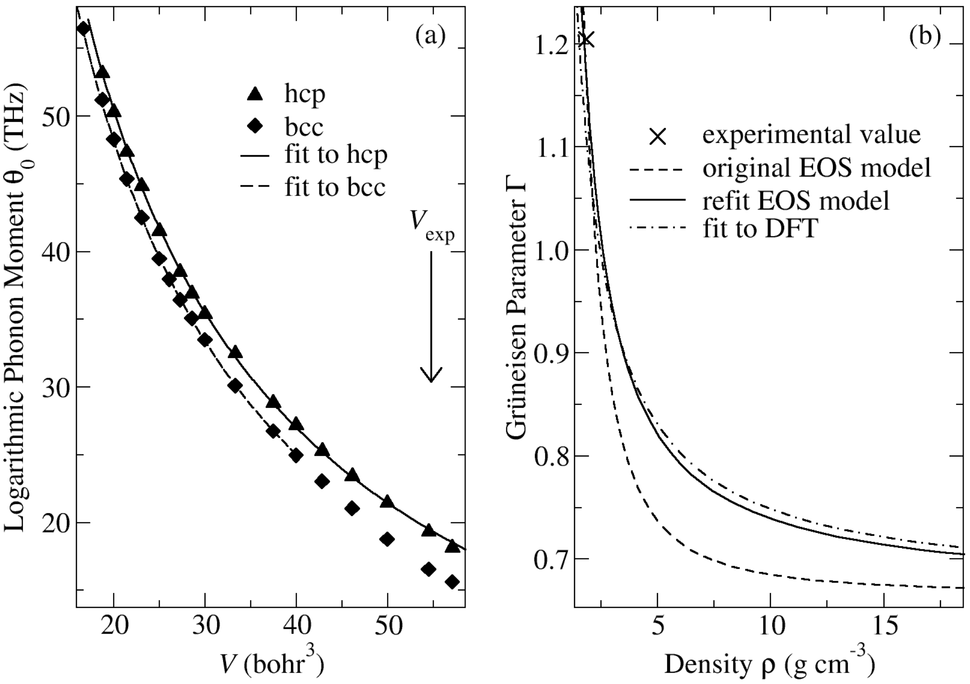

Figure 4. (a) Calculated logarithmic phonon moments for the hcp and bcc structures as function of volume. (b) Grüneisen parameter for hcp Be.

Figure 5 shows the hcp to bcc structural phase transition predicted by the calculations presented here. Based on the cold curves the transition occurs at 415 GPa for the FP-LMTO and PAW calculations and at 440 GPa for the APW+lo calculations. This difference is likely to be due to the different treatment of the 1*s* electron. The inclusion of the effect of zero point energy from the phonons (calculated using the PAW method) raises the zero temperature transition by about 30 GPa.

With increasing temperature the relative stability changes in favor of the bcc crystal structure, as expected from the lower phonon moment of the bcc structure relative to the hcp value. The slope of the transition line levels off to a constant value in the range of 800 K. This is the temperature range in which all phonon states have been occupied. Anharmonic effects outside the scope of the quasiharmonic approximation, i.e., phonon-phonon interactions, start to become important at these high temperatures. The absence of these effects is evident in the absence of melting in the quasiharmonic approximation. The experimentally observed temperature-induced phase transition from hcp to bcc at ambient pressure occurs at temperatures very close to melting. Since the quasiharmonic approximation breaks down at these temperatures the calculated hcp to bcc phase transition at ambient pressure is not adequately described.

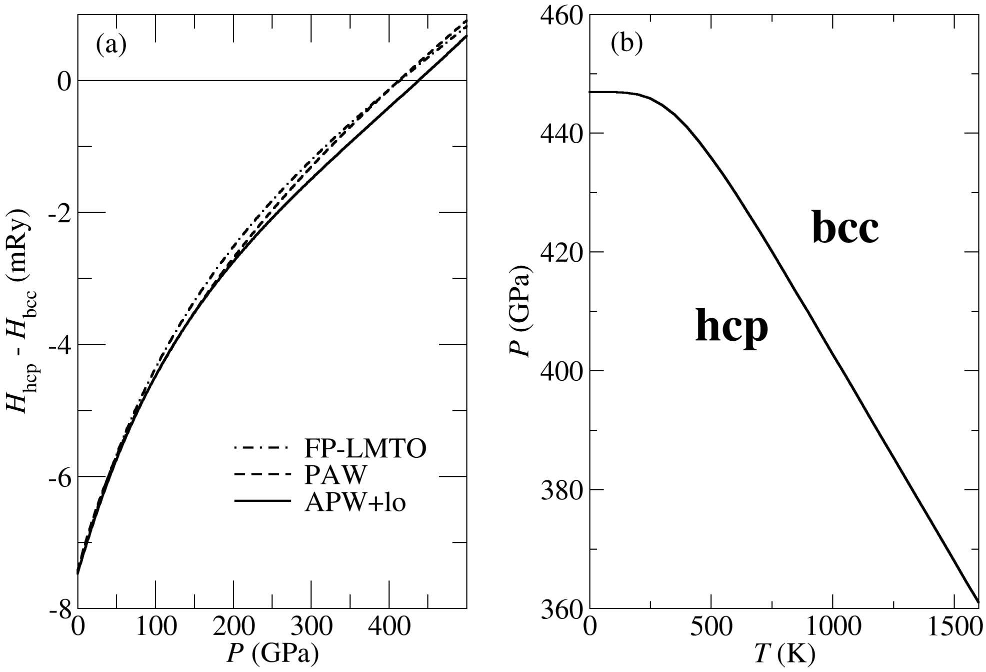

Figure 5. (a) Differences in the enthalpies between the two structures in the three methods. The predicted phase transition from hcp to bcc based on the cold curves (without zero-point energy) is at 415 GPa for FP-LMTO and PAW and at 440 GPa for APW+lo (where the 1*s* electrons are treated differently). (b) Predicted phase transition line for beryllium in the quasiharmonic approximation. The temperature dependence is determined by the phonons and is only valid at temperatures well below melting (1560 K).

Discussion

An anomalous behavior of the Grüneisen parameter as a function of density, as suggested by recent diamond anvil cell experiments (Velisavljevic *et al.*, 2002), is not supported by the calculations presented here. The phonon frequencies stiffen with increasing pressure in a smooth, monotonic fashion. We note that Velisavljevic *et al.* did not use a pressure medium in the experimental set up for the highest pressure data points. The cold curve as well as the phonon moments and the Grüneisen parameter calculated here do, on the other hand, agree very well with the EOS model extracted from shock experiments.

Agreement with experiment is also found in predicting a pressure-induced, low-temperature hcp to bcc structural phase transition. The calculations presented here place this transition at pressures well above the highest pressure achieved in (static) experiments in which no transition was observed. This disagrees with earlier, more approximate calculations based on DFT, suggesting that the approximations used in those calculations were too severe for the case of beryllium. In particular, the earlier calculations do not optimize the c/a ratio for hcp Be at each volume. We find that without this optimization the hcp to bcc transition would be significantly lower.

On the other hand, the observed temperature-induced, low-pressure hcp to bcc structural phase transition is absent in the results calculated here. This transition occurs at temperatures close to melting, i.e., at temperatures where the quasiharmonic approximation looses its validity.

Conclusion

Using three different augmented wave DFT methods the EOS of beryllium was calculated and compared with previous experimental and theoretical data. Results from the three methods agree very well with each other. Energy differences on the order of one mRy appear at high pressures. Treating the 1*s* electrons as core instead of valence electrons affects the calculated hcp-bcc structural phase transition pressure by about 5%. The calculated pressure is somewhat over 400 GPa, more than twice the highest pressure in experiments that did not find such a transition.

Using the direct force method the phonons were calculated for the hcp and bcc crystal structures. In the hcp structure good agreement is found with the experimentally measured phonon dispersion and thermal expansion. The calculated Grüneisen parameter is also very close to the model used to fit shock experiments.

Two discrepancies remain between the calculated results and experiment. The calculations do not predict a low-pressure hcp-bcc phase transition at temperatures just below melting, this failure is attributed to the quasiharmonic approximation which is not valid near melting. The calculations also do not reveal any anomalous behavior in the Grüneisen parameter as would be necessary to fit recent diamond anvil data, which is attributed to uncertainties resulting from the lack of a pressure medium in those experiments.

Acknowledgement

We thank Carl Greeff and John Wills for helpful and encouraging discussions. This research is supported by the U.S. Department of Energy under Contract No. W-7405-ENG-36.

References

BLAHA, P., SCHWARZ, K, MADSEN, G.K.H., KVASNICKA, D., AND LUITZ, J., 2001. *WIEN2K, an augmented plane wave + local orbitals program for calculating crystal properties*. Wien: Karlheinz Schwartz, Technische Universität.

BLÖCHL, P., JEPSEN, O., AND ANDERSON, O.K., 1994. Improved tetrahedron method for Brillouin-zone integration. *Phys. Rev. B*, 49 (23), 16223-16233.

BLÖCHL, P., 1994. Projector augmented-wave method. *Phys. Rev. B*, 50, 17953.

FRANK, W., ELSÄSSER, C., and FÄHNLE, M., 1995. Ab initio Force-Constant Method for Phonon Dispersions in Alkali Metals. *Phys. Rev. Lett.*, 74 (10), 1791-1794.

KRESSE, G. AND FURTHMÜLLER, J., 1996. Efficient iterative schemes for ab initio total-energy calculations using a plane-wave basis set. *Phys. Rev. B*, 54 (16), 11169-11186.

KRESSE, G. AND JOUBERT, J., 1999. From ultrasoft pseudopotentials to the projector augmented wave method. *Phys. Rev. B*, 59, 1758.

KUNC, K. and MARTIN, R.M., 1982. Ab Initio Force Constants of GaAs: A New Approach to Calculation of Phonons and Dielectric Properties. *Phys. Rev. Lett.*, 48 (6), 406-409.

LAM, P.K., CHOU, M.Y., AND COHEN, M.L., 1984. Temperature- and pressure-induced crystal phase transitions in Be. *J. Phys. C: Solid State Phys.*, 17, 2065-2073.

LYON, S. P. AND JOHNSON, J. D., 1998. *T-1 Handbook of the Sesame Equation of State Library*. Los Alamos: Los Alamos National Laboratory.

MARSH, S.P., 1980. *LASL shock Hugoniot data*. Berkeley: University of California Press, 21.

MCMAHAN, A.K., 1982. The □–□ transition in T=0 high pressure beryllium. *AIP Conf. Proc.*, 78, 340-344.

MCQUEEN, R.G., MARSH, S.P., TAYLOR, J.W., FRITZ, J.N., AND CARTER, W.J., 1970. The equation of state of solids from shock wave studies. *In*: R. KINSHAW, ed. *High-velocity impact phenomena*. New York: Academic Press, 293, and references therein.

MING, L.C. AND MANGHNANI, M.H., 1984. Isothermal compression and phase transition in beryllium to 28.3 GPa. *J. Phys. F: Met. Phys*., 14, L1-L8.

NAKANO, K., AKAHAMA, Y., AND KAWAMURA, H., 2002. X-ray diffraction study of Be to megabar pressure. *J. Phys.: Cond. Mat*., 14 (44), 10569-10573.

OLIJNYK, H. AND JEPHCOAT, A.P., 2000. Raman spectra of beryllium to 23 GPa. *J. Phys. Cond. Mat.*, 12 (41), 8913-8918.

PARLINSKI, K., LI, Z.Q., and KAWAZOE, Y., 1997. First-Principles Determination of the Soft Mode in Cubic ZrO2. *Phys. Rev. Lett*., 78 (21), 4063-4066.

PATHRIA, R.K., 1972. *Statistical mechanics*. Oxford: Pergamon, 76-139.

PERDEW, J.P., 1991. Generalized gradient approximation. *In*: P. ZIESCHE AND H. ESCHRIG, eds. *Electronic Structure of Solids '91*. Berlin: Akademie Verlag, 11.

PERDEW, J.P., BURKE, S., AND ERNZERHOF, M., 1996. Generalized gradient approximation made simple. *Phys. Rev. Lett*., 77 (18), 3865-3868.

PRICE, D.L. AND COOPER, B.R., 1989. Total energies and bonding for crystallographic structures of titanium-carbon and tungsten-carbon systems. *Phys. Rev. B*, 39 (8), 4945.

VELISAVLJEVIC, N., CHESNUT, G. N., VOHRA, Y. K., WEIR, S. T., MALBA, V., AND AKELLA, J., 2002. Structural and electrical properties of beryllium metal to 66 GPa studied using designer diamond anvils. *Phys. Rev. B*, 65, 172107.

WILLS, J.M. AND COOPER, B.R., 1987. Synthesis of band and model Hamiltonian theory for hybridizing cerium system. *Phys. Rev. B*, 36, 3809.

WILLS, J.M., ERIKSSON, O., ALOUANI, M., AND PRICE, D. L., 2000. Full-potential LMTO total energy and force calculations. *In*: H. DREYSSE, ed. *Lecture notes in physics*, 535. Berlin: Springer Verlag, 148-167.

WEI, S. AND CHOU, M.Y., 1992. Ab initio calculation of force constants and full phonon dispersions. *Phys. Rev. Lett*., 69 (19), 2799-2802.